Electron Transport in 4*H*-1,1-Dioxo-4-(dicyanomethylidene)thiopyrans. Investigation of X-ray Structures of Neutral Molecules, Electrochemical Reduction to the Anion Radicals, and Absorption Properties and EPR Spectra of the Anion Radicals

Michael R. Detty,*,† Raymond S. Eachus,‡ John A. Sinicropi,† Jerome R. Lenhard,‡ Martin McMillan,§,⊥ Anne Marie Lanzafame,§ Henry R. Luss,§ Ralph Young,† and James E. Eilers||

Office Imaging Research and Technical Development, Eastman Kodak Company, Rochester, New York 14650-2129, Imaging Research and Advanced Development, Eastman Kodak Company, Rochester, New York 14650, Analytical Technology Division, Eastman Kodak Company, Rochester, New York 14652-3712, and Research Technology Support Services, Eastman Kodak Company, Rochester, New York 14650

Received October 24, 1994®

A series of 4*H*-1,1-dioxo-4-(dicyanomethylidene)thiopyrans **1**–**15**, which are useful as electron-transport materials in xerography, were prepared by condensation of malononitrile with the corresponding 4*H*-1,1-dioxothiopyran-4-one. X-ray crystal structures of **1**–**5** were indicative that the thiopyran ring is planar in **1**, **2**, and **5** and is boat shaped in the *tert*-butyl-substituted derivatives **3** and **4**. The 2-thienyl substituent in **5** is rigorously coplanar with the thiopyran ring in **5**. The anion radicals of **1**–**6**, which were prepared by electrochemical or lithium naphthalenide reduction, were examined by EPR and absorption spectroscopy. The experimental spin densities as determined at atomic centers by EPR spectroscopy are consistent with values determined by an *ab initio* calculation on the anion radical of **9**. The reduction potentials of **1**–**15** as measured by second-harmonic AC voltammetry (SHACV) correlated with the sum of Hammett substituent constants at the 2- and 6-positions. Coulometric reduction and reoxidation was indicative of reversible one-electron processes in these systems. Parent compound **2** gave completely irreversible reduction even by SHACV. Electron mobilities of thin films of **3**, **4**, or **15** molecularly dispersed in a polyester binder were found to increase with increased planarity of the electron-transport material and increased π-delocalization of the unpaired spin.

Introduction

One format for configuring photoconductive materials useful in xerography is shown in Figure 1 with a discrete charge generation layer (CGL) and a discrete charge transport layer (CTL).[1] Typically, 400–600 V is applied across a 10–20-μm-thick film, which leads to fields on the order of 5×10^5 V cm^{-1}. The resulting capacitor can be discharged upon exposure to light by creating hole-electron pairs, which render the exposed areas conductive. In the configuration shown in Figure 1, the CGL injects electrons into the CTL upon exposure to light of appropriate wavelengths. Typically, the CTL consists of a molecularly doped polymer while the CGL contains a thin layer of a photosensitive compound such as an organic pigment or amorphous selenium. The charge-transport phenomenon in the CTL prevents recombination of holes and electrons by moving electrons to the positive face of the capacitor. The rate at which electrons are transported in the CTL is defined as the mobility, μ, of the layer and is a function of both the thickness of the film and the applied field. The intrinsic mobility of the photoconductive film package limits both the quantum yield for photodischarge (by allowing recombination) and the process speed for developing and transferring the image in xerographic applications. Typically, the CGL is much thinner than the CTL such that mobilities in the CGL are less important than those of the CTL.

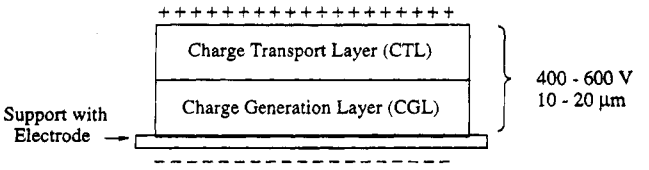

Figure 1. Cross section of a photoconductive film configured for electron transport in the CTL.

The number of electron-transport materials useful in xerographic applications remains small. 2,4,7-Trinitro-9-fluorenone (TNF)[2] and 7,7,8,8-tetracyano-1,4-quinodimethane (TCNQ)[3] are two examples of electron transport materials with limited miscibility in polymeric binders. Alkylated derivatives of TNF have been described with improved miscibility in polymers.[4] Numerous efforts have extended the π-framework of the TCNQ

* Current address: Dept. of Medicinal Chemistry, School of Pharmacy, SUNY at Buffalo, Buffalo, NY 14260.
† Office Imaging Research and Technical Development.
‡ Imaging Research and Advanced Development.
§ Analytical Technology Division.
|| Research Technology Support Services.
⊥ Author to whom correspondence should be addressed regarding X-ray structural data.
® Abstract published in *Advance ACS Abstracts,* March 1, 1995.
(1) (a) Schein, L. B. *Electrophotography and Development Physics*; Springer: New York, 1988. (b) Borsenberger, P. M.; Weiss, D. S. *Organic Photoreceptors for Imaging Systems*; Marcel Dekker: New York, 1993.

(2) (a) Gill, W. D. *J. Appl. Phys.* **1972**, *43*, 5033. (b) Gill, W. D. In *Amorphous and Liquid Semiconductors*; Stuke, J., Brenning, W., Eds.; Taylor and Francis: London, 1973; p 901.
(3) (a) Cairns, T. L.; McKusick, B. C. *Angew. Chem.* **1961**, *73*, 520. Acker, D. S.; Hertler, W. R. *J. Am. Chem. Soc.* **1962**, *84*, 3370. (b) Ferraris, J.; Cowan, D. O.; Walatka, V. V.; Perlstein, J. H. *J. Am. Chem. Soc.* **1973**, *95*, 948.

0022-3263/95/1960-1674$09.00/0

molecule[5,6] while other efforts have included placing additional electron-withdrawing groups around the TCNQ nucleus.[6,7] These materials are sparingly soluble as well. Diphenoquinone (DPQ) derivatives have been described as nonmutagenic (Ames test), electron-transport materials.[8] The limited miscibility of the electron-transport materials in polymeric binders has hindered physical-organic studies of structure and mobility.

Charge transport in polymeric systems has been discussed in terms of the Bässler formalism,[9] which states that a molecular crystal is split into a Gaussian distribution of localized states because of the lack of long-range order in polymers. The formalism, which was developed largely by Monte Carlo techniques, is based on fluctuations of site energies and intersite distances. This formalism suggests that both electronic and steric effects of substituents should be important in structure–mobility studies of charge-transport materials.[9g]

The Y-shaped geometry of the dicyanomethylidene group has imposed steric constraints on substituent choices in the TCNQ-class of molecules. The planar nature of TCNQ and its anion radical are thought to be important in the high conductivity of complexes of TCNQ since metallic character has not been described in complexes of nonplanar analogues of TCNQ. TCNQ analogues based on naphthoquinone,[10] anthraquinone,[11] and other tetrasubstituted TCNQ derivatives[12] have boat-shaped carbon skeletons for the dicyanomethylidene-bearing ring. The cyanoimine functionality has been introduced as a more flexible version of the dicyanomethylidene moiety with similar electronic properties,[13,14] and acceptors containing this functionality form highly conductive anion radical complexes.[15–18]

4H-1,1-Dioxo-4-(dicyanomethylidene)-2,6-diphenylthiopyran (**1**), has been described as a sulfone-containing analogue of TCNQ[19] and has been utilized as an electron-transport material in electrophotographic applications.[20] In the preceding manuscript, synthetic routes for the preparation of 4H-thiopyran-4-one 1,1-dioxides with a variety of substituents at the 2- and 6-positions were described.[21] We have converted these materials to the corresponding dicyanomethylidene derivatives and, herein, describe the steric and electronic effect of substituents at the 2- and 6-positions on the chemistry and spectroscopy of the 4H-1,1-dioxo-4-(dicyanomethylidene)thiopyrans **1**–**15** and their anion radicals as well as on the mobility of electrons in the molecularly doped polymers containing them.

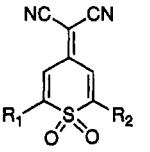

1, $R_1 = R_2$ = Ph
2, $R_1 = R_2$ = H
3, $R_1 = R_2$ = *tert*-Bu
4, R_1 = Ph, R_2 = *tert*-Bu
5, R_1 = Ph, R_2 = 2-thienyl
6, $R_1 = R_2$ = 2-thienyl
7, $R_1 = R_2$ = 3-thienyl
8, $R_1 = R_2$ = 2-furyl
9, $R_1 = R_2$ = Me
10, R_1 = Me, R_2 = Ph
11, R_1 = *tert*-Bu, R_2 = 2-thienyl
12, R_1 = Ph, R_2 = 3-thienyl
13, R_1 = Ph, R_2 = 2-furyl
14, R_1 = Ph, R_2 = *n*-Bu
15, R_1 = Ph, R_2 = *p*-tolyl

Results and Discussion

Preparation of 4H-1,1-Dioxo-4-(dicyanomethylidene)thiopyranone. 2,6-Diaryl or heteroaryl derivatives **1**, **5**–**8**, **12**, **13**, and **15** were prepared by the condensation of malononitrile with the corresponding 4H-thiopyran-4-one 1,1-dioxide using catalytic piperidine in ethanol. This procedure did not work as well for the preparation of the parent 4H-1,1-dioxo-4-(dicyanomethylidene)thiopyran (**2**) or with alkyl- or dialkyl-substituted derivatives **3**, **4**, **9**–**11**, and **14**. In the alkyl-substituted systems, hydrolysis of one nitrile to an amide functionality was observed as a significant side reaction. The condensation of malononitrile with alkyl-substituted 4H-thiopyran-4-one 1,1-dioxides in dichloromethane using basic alumina gave good yields of the dicyanomethylidene products free from amide contamination.

X-ray Crystal Structures of 1–5. The substituents at the 2- and 6-positions in **1**–**15** encompass a wide range of steric and electronic parameters. Steric effects in both the neutral molecules and the anion radicals of **1**–**15** should be similar and might influence the packing of the transport molecules in the polymer as well as the delocalization of spin in open-shell systems. While stacking in molecular solids might be greatly affected by a lack of planarity in these molecules, electronic effects

(4) (a) Ong, B. S.; Keoshkerian, B.; Martin, T. I.; Hamer, G. K. *Can. J. Chem.* **1985**, *63*, 147. (b) Loutfy, R. O.; Ong, B. S. *Can. J. Chem.* **1984**, *62*, 2546. (c) Loutfy, R. O.; Ong, B. S.; Tadros, J. *J. Imag. Sci.* **1985**, *29*, 69. (d) Murti, D. K.; Kazmaier, P. M.; DiPaola-Baranyi, G.; Hsiao, C. K.; Ong, B. S. *J. Phys. D* **1987**, *20*, 1606. (e) Murti, D. K.; Murray, H.; Baillie, S. *J. Phys. D* **1986**, *19*, 1265.

(5) Chatterjee, S. *J. Chem. Soc.* **1967**, 1170. Diekmann, J.; Hertler, W. R.; Benson, R. E. *J. Org. Chem.* **1963**, *28*, 2719. Sandman, D. J.; Garito, A. F. *J. Org. Chem.* **1974**, *39*, 1165. Addison, A. W.; Dalal, N. S.; Hoyano, Y.; Huizinga, S.; Weiler, I. *Can. J. Chem.* **1977**, *55*, 4191. Aharon-Shalom, E.; Becker, J. Y.; Agranat, I. *Nouv. J. Chim.* **1979**, *3*, 643. Maxfield, M. R.; Cowan, D. O.; Bloch, A. N.; Poehler, T. O. *Nouv. J. Chim.* **1979**, *3*, 647. Maxfield, M. R.; Willi, S. M.; Cowan, D. O.; Bloch, A. N.; Poehler, T. O. *J. Chem. Soc., Chem. Commun.* **1980**, 947. Acton, N.; Hou, D.; Schwartz, J.; Katz, T. J. *J. Org. Chem.* **1982**, *47*, 1011.

(6) For EPR spectra of these materials: Gerson, F.; Heckendorn, R.; Cowan, D. O.; Kini, A. M.; Maxfield, M. *J. Am. Chem. Soc.* **1983**, *105*, 7017 and references cited therein.

(7) Wheland, R. C.; Martin, E. L. *J. Org. Chem.* **1975**, *40*, 3101.

(8) (a) Yamaguchi, Y.; Tanaka, H.; Yokoyama, M. *J. Chem. Soc., Chem. Commun.* **1990**, 222. (b) Yamaguchi, Y.; Yokoyama, M. *Chem. Mater.* **1991**, *3*, 709.

(9) (a) Bässler, H. *Phys. Status Solidi (b)* **1981**, *107*, 9. (b) Bässler, H. *Philos. Mag. B* **1984**, *50*, 347. (c) Bässler, H. *Prog. Coll. Polym. Sci.* **1989**, *80*, 35. (d) Bässler, H. In *Optical Techniques to Characterize Polymer Systems*; Bässler, H., Ed.; Elsevier: Amsterdam, 1989; p 181. (e) Bässler, H. In *Hopping and Related Phenomena*; Fritzsche, H., Pollak, M., Eds.; World Scientific: Singapore, 1990; p 491. (f) Bässler, H. *Phys. Status Solidi (b)* **1993**, *175*, 15. (g) Borsenberger, P. M.; Detty, M. R.; Magin, E. H. *Phys. Status Solidi (b)* **1994**, *185*, 465.

(10) Iwasaki, F. *Acta Crystallogr.* **1971**, *B27*, 1360.

(11) Schubert, U.; Hünig, S.; Aümuller, A. *Liebigs Ann. Chem.* **1985**, 1216.

(12) (a) Rosenau, B.; Krieger, C.; Staab, H. A. *Tetrahedron Lett.* **1985**, *26*, 2081. (b) Silverman, J.; Yannoni, N. F. *J. Chem. Soc. (B)* **1967**, 194.

(13) Hünig, S. *Pure Appl. Chem.* **1990**, *62*, 395.

(14) Aumüller, A.; Hünig, S. *Angew. Chem., Int. Ed. Engl.* **1984**, *23*, 447.

(15) Aumüller, A.; Erk, P.; Klebe, G.; Hünig, S.; von Schutz, J. U.; Werner, H.-P. *Angew. Chem., Int. Ed. Engl.* **1986**, *25*, 740. Erk, P.; Klebe, G.; Hünig, S.; von Schutz, J. U.; Werner, H.-P.; Wolf, H. C. *Ibid.* **1988**, *27*, 267.

(16) Gerson, F.; Gescheidt, G.; Mockel, R.; Aumüller, A.; Erk, P.; Hünig, S. *Helv. Chim. Acta* **1988**, *71*, 1665.

(17) Bryce, M. R.; Davies, S. R.; Grainger, A. M.; Hellberg, J.; Hursthouse, M. B.; Mazid, M.; Bachmann, R.; Gerson, F. *J. Org. Chem.* **1992**, *57*, 1690.

(18) de la Cruz, P.; Martin, N.; Miguel, F.; Seoane, C.; Albert, A.; Cano, F. H.; Gonzalez, A.; Pingarron, J. M. *J. Org. Chem.* **1992**, *57*, 6192.

(19) Chen, C. H.; Reynolds, G. A.; Luss, H. R.; Perlstein, J. H. *J. Org. Chem.* **1986**, *51*, 3282.

(20) (a) Scozzafava, M.; Chen, C. H.; Reynolds, G. A.; Perlstein, J. H. U.S. Patent 4,514,481 (1985). (b) Rule, N. G.; Kung, T.-M. U.S. Patent 5,039,585 (1991).

(21) Rule, N. G.; Detty, M. R.; Kaeding, J. E.; Sinicropi, J. A. *J. Org. Chem.* **1995**, *60*, 1665.

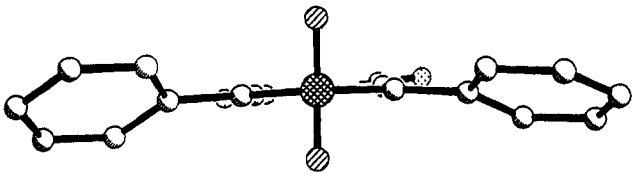

Figure 2. A ball-and-stick model of the molecule **1** as viewed in the plane of the central ring through the sulfone group.

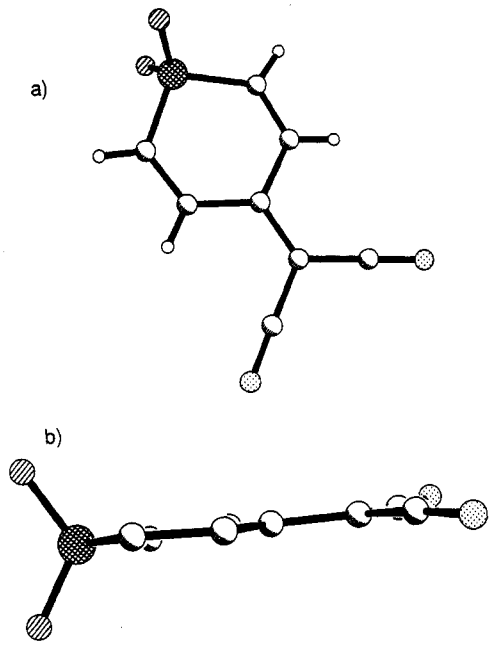

Figure 3. Views from the (a) top of the ball-and-stick model of **2** and (b) from the side of the molecule.

from nonplanarity should fall off with cos θ where θ represents the dihedral angle between the plane of the central thiopyran ring and the plane of the substituent.

X-ray crystallographic analysis of single crystals of **1** has been described.[19] We have examined the refinement of these data and describe minor corrections in the reported values. The thiopyran ring in **1** is approximately planar with small deviations of between −0.030 and +0.041 Å from the least-squares plane (Figure 2). The plane of the dicyanomethylidene moiety is slightly bent at 3.5° (although this angle and similar angles described for **2**–**5** are actually complex angles, the bend is large relative to the twist) from the plane of the sulfone-containing ring while the two phenyl groups form dihedral angles of 31.0° and −23.6°,[22] respectively, with the thiopyran ring. Presumably, steric interactions between the *ortho*-hydrogens of the phenyl rings on the 2- and 6-positions of the thiopyran ring and both the oxygen atoms of the sulfone group and the hydrogen atoms at positions 3 and 5 of the thiopyran ring are responsible for the large dihedral angles.

A planar central ring was also found in the X-ray crystallographic analysis of the parent sulfone **2** as shown in Figure 3. The atoms of the thiopyran ring have deviations of between −0.013 and +0.013 Å from the least-squares plane. As observed in **1**, the plane of the dicyanomethylidene moiety is bent slightly at 4.7° from the plane of the ring.

(22) In ref 19, dihedral angles of 31.1° and −33.1° were reported. The second value is in error. The correct value for the refinement in ref 16 is −23.6°.

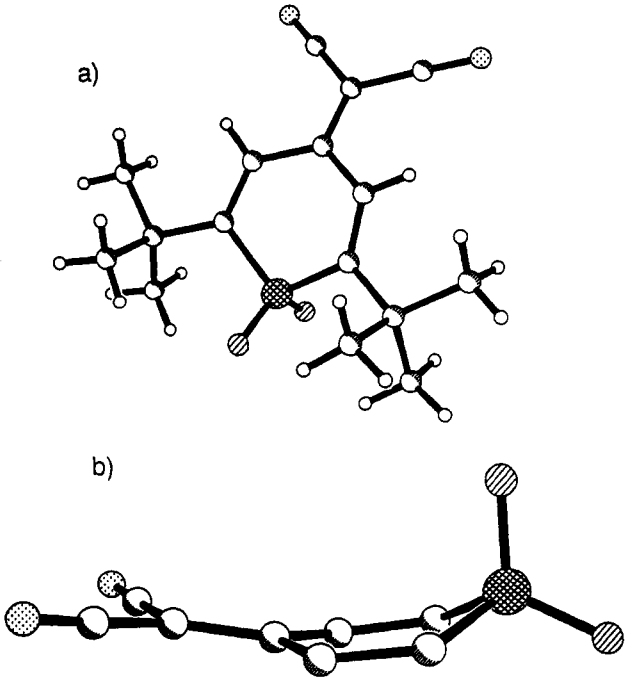

Figure 4. Views from (a) the top of the ball-and-stick model of **3** and (b) from the side with the *tert*-butyl groups removed for clarity.

Steric effects from bulky *tert*-butyl substituents gave quite different geometries for **3** and **4**. X-ray crystallographic analysis of a single crystal of **3** was indicative of a nonplanar central ring as shown in Figure 4. The sulfone-containing ring is boat-shaped to relieve steric interactions with dihedral angles of 23.9° and 15.0° for the bow plane containing the thiopyran sulfur atom and the stern plane containing the carbon bearing the dicyanomethylidene group with the plane defined by the four central carbon atoms, respectively. The dihedral angle of the plane of the dicyanomethylidene moiety with plane defined by the stern of the thiopyran boat is 5.5°.

Sulfone, **4**, bearing one *tert*-butyl substituent and one phenyl substituent, is not as severely distorted from planarity as **3** as shown in Figure 5. The central ring is slightly boat-shaped with dihedral angles of 12.2° and 7.4° for the bow plane containing the sulfone sulfur atom and the stern plane containing the carbon bearing the dicyanomethylidene group with the plane defined by the four central carbon atoms, respectively. The plane of the dicyanomethylidene moiety is bent 3.2° from the plane defined by the stern of the thiopyran ring. The dihedral angle of the phenyl ring and the plane defined by the four central carbon atoms of the sulfone-containing ring is 29.8°.

The comparison of the geometries of the phenyl and 2-thienyl substituents of **5** reveals some interesting differences. Single-crystal X-ray crystallographic analysis of **5** gave the structure shown in Figure 6. The central thiopyran ring is planar with small deviations of between −0.011 and +0.012 Å from the least-squares plane. The plane of the dicyanomethylidene moiety is bent 5.7° with respect to the thiopyran ring. The most interesting feature of this structure is the observation that the 2-thienyl substituent and the thiopyran ring are coplanar with less than 1° of twist. The 2-thienyl substituent, as a five-membered ring and with the substitution of a sulfur atom for a CH-group, minimizes steric interactions with the hydrogen atom at the 3-position of the thiopyran

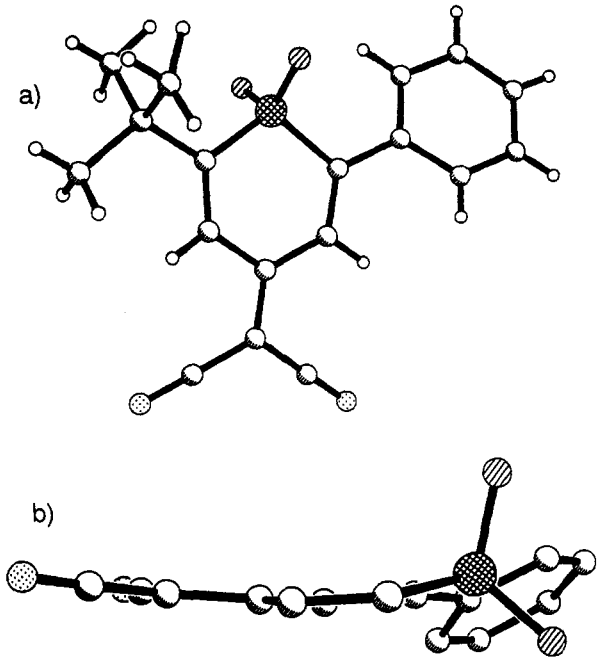

Figure 5. Views from (a) the top of the ball-and-stick model of **4** and (b) from the side with the *tert*-butyl group removed for clarity.

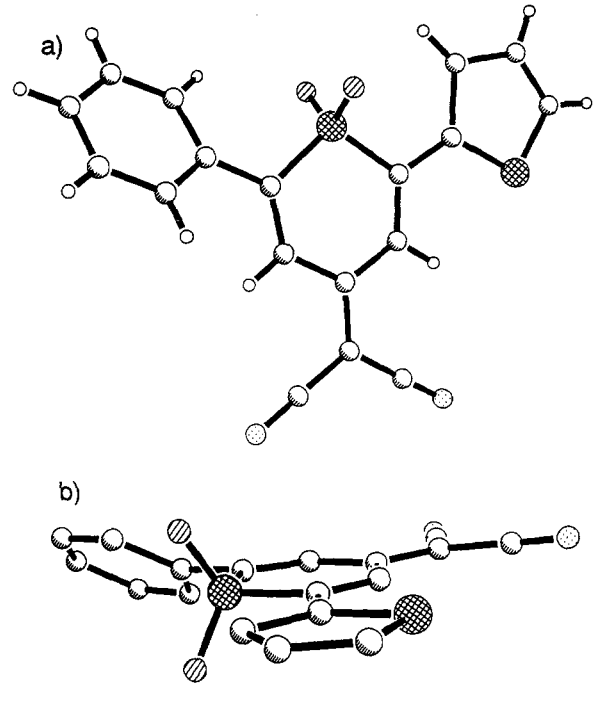

Figure 6. Views from (a) the top of the ball-and-stick model of **5** and (b) from the side.

ring relative to a phenyl group. This observation can be contrasted with the steric interactions still present between the *ortho*-hydrogens of the phenyl substituent and the hydrogen atom at the 5-position of the thiopyran ring in **5**. The dihedral angle formed by the plane of the phenyl substituent and the plane of the thiopyran ring is 36.6°.

Reduction Potentials of Sulfones 1–15. One measure of substituent effects in **1–15** might be the substituent-induced changes in reduction potentials. Cyclic voltammetry experiments conducted in acetonitrile at a potential scan rate of 0.1 V s^{-1} indicate that the one-electron reductions for **1**, **4–8**, and **11–15** are reversible, whereas the reductions of **3**, **9**, and **10** are quasireversible. In contrast, the reduction process for the parent sulfone **2** is irreversible at potential scan rates ranging from 0.02 V s^{-1} to 1000 V s^{-1}. In order to avoid these chemical complications, the one-electron reduction potentials, $E^{\circ 1}$, were measured by the method of second-harmonic AC voltammetry (SHACV)[23] and are compiled in Table 1.

Table 1. Reduction Potentials for Sulfones 1–15 in Acetonitrile[a]

compd	R_1	R_2	$E^{\circ 1}$,[a] V vs SCE	$E^{\circ 2}$, V vs SCE	ΔE°, V	σ_{sum}[b]
1	Ph	Ph	−0.203	−0.832	0.63	0.10
2	H	H	−0.215	–	–	0.00
3	*tert*-Bu	*tert*-Bu	−0.394	−1.2[c]	0.81	−0.30
4	Ph	*tert*-Bu	−0.288	−0.975	0.69	−0.10
5	Ph	2-thienyl	−0.185	−0.795	0.59	0.10
6	2-thienyl	2-thienyl	−0.171	−0.759	0.59	0.10
7	3-thienyl	3-thienyl	−0.229	−0.850	0.62	−0.04
8	2-furyl	2-furyl	−0.175	0.80[c]	−0.63	0.04
9	Me	Me	−0.395	−1.2[c]	–	−0.28
10	Me	Ph	−0.283	−0.88[c]	0.60	−0.09
11	*tert*-Bu	2-thienyl	−0.21[d]	−0.81	0.60	−0.10
12	Ph	3-thienyl	−0.224	−0.850	0.63	0.03
13	Ph	2-furyl	−0.186	−0.800	0.61	0.07
14	Ph	*n*-Bu	−0.288	−0.975	0.69	−0.08
15	Ph	*p*-tolyl	−0.219	−0.855	0.69	0.10

[a] By SHACV at a scan rate of 50 mV s^{-1} and frequency of 400 Hz at a Pt disk electrode in acetonitrile with 0.1 M tetra-*n*-butylammonium tetrafluoroborate as supporting electrolyte. Sample concentration was 0.5–1.0 × 10^{-4} M. [b] Sum of Hammett substituent constants for R_1 and R_2. [c] Peak potential of irreversible reduction. [d] By conventional cyclic voltammetry with a scan rate of 0.1 V s^{-1} at a Pt disk electrode in acetonitrile with 0.1 M tetra-*n*-butylammonium tetrafluoroborate as supporting electrolyte.

With the exception of compound **2**, these sulfones also accept a second electron at applied potentials ranging from −0.75 to −1.2 V to generate the sulfone dianions. The dianions for all of the sulfones were considerably less stable than the corresponding anion radical species. In acetonitrile, the addition of a second electron was found to be fully reversible only for sulfones **1**, **5**, **6**, **12**, **13**, and **15**. This second reduction process is quasireversible (ΔE_p > 100 mV) for **3**, **4**, and **7** and chemically irreversible for the remaining sulfones of Table 1.

Substituent Effects on Reduction Potentials in Thiopyran Sulfones. Electrochemical values of $E^{\circ 1}$ should reflect thermodynamic differences in energies (ΔG) between the neutral sulfones and their anion radicals. The changes observed in reduction potentials from substituent changes correlate well with the sum of Hammett substituent constants for the groups at positions 2 and 6. Hammett σ_p values are −0.15 for *tert*-butyl, −0.14 for methyl, 0.00 for hydrogen, and 0.05 for phenyl.[24] Hammett σ_p values of 0.02 for 2-furyl,[24] 0.05 for 2-thienyl,[25] and −0.02 for 3-thienyl[25] have also been measured. Because the 2- and 6-substituents are on pseudosymmetric sites of the pentadienyl fragment of the sulfone anion radicals, substituent effects should be roughly additive.

Sums of the Hammett σ_p constants for the 2,6-substituents in each of the compounds **1–15** are compiled in

(23) Lenhard, J. *J. Imag. Sci.* **1986**, *30*, 27.
(24) Exner, O. In *Correlation Analysis in Chemistry: Recent Advances*; Chapman, N. B., Shorter, J., Eds.; Plenum Press: New York, 1978.
(25) Fringuelli, F.; Marino, G.; Taticchi, A. *J. Chem. Soc. (B)* **1971**, 2302.

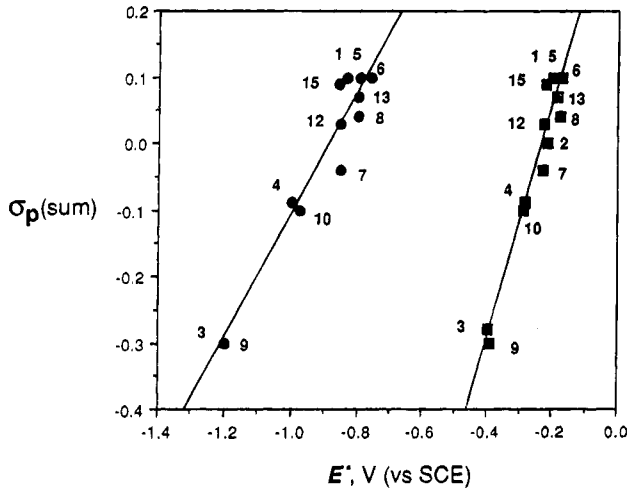

Figure 7. A plot of the sum of σ_p-values for Hammett substituent constants at the 2- and 6-positions of 1,1-dioxothiopyrans **1**−**15** as a function of reduction potential ($E°$) for both the first and second reductions of these systems. For the first reduction, $R^2 = 0.94$, the slope = 1.75, and the intercept = 0.40. For the second reduction, $R^2 = 0.91$, the slope = 0.91, and the intercept = 0.82.

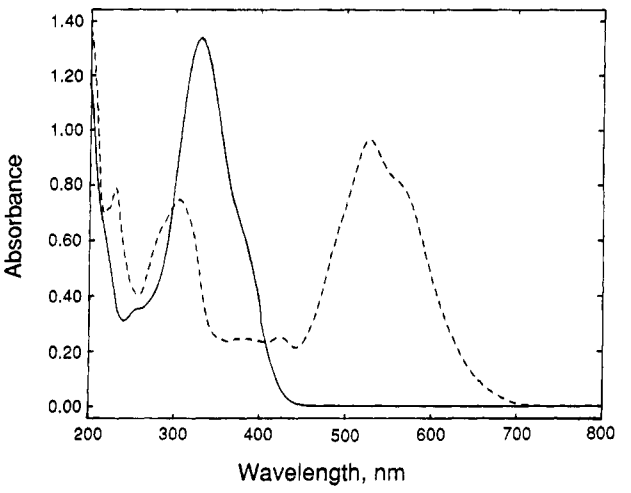

Figure 8. Absorption spectra of sulfone **4** (—) and its anion radical (- - -) in acetonitrile.

Table 1. A plot of reduction potential E^{o1} as a function of the sum of substituent constants [σ_p (sum)] is linear with a slope of 1.75 ($R^2 = 0.94$) as shown in Figure 7. These data are consistent with both inductive and resonance effects from substituents being important in the stabilization of the anion radicals. The reduction potential for the addition of a second electron is also linearly related to the sum of the substituent constants as shown in Figure 7 with a slope of 0.92 ($R^2 = 0.91$). This smaller slope is consistent with increased sensitivity to substituent effects for the formation of the dianion from the anion radical.

Electrochemical Generation and Absorption Spectra of Sulfone Anion Radicals in Acetonitrile. Solutions of sulfone anion radical were prepared for spectroscopic examination using either a three-compartment bulk electrolysis cell or a tubular flow-cell. Bulk electrolysis experiments were conducted at a potential 200 mV negative of E^{1o} (as listed in Table 1) giving complete reduction to the anion within a few minutes. Utilization of the flow-cell under conditions of high-flow rate (20 mL/min) allowed for spectral measurements to be made several seconds after formation of the sulfone radical ion. Spectra obtained using the flow-cell were identical to those recorded during bulk-electrolysis experiments. The reduction products exhibit spectral absorption at longer wavelengths than their respective neutral parent compounds as shown in Figure 8 for $\mathbf{4}^-$ and in Figures 15−18 of the supplementary material for $\mathbf{1}^-$−$\mathbf{3}^-$ and $\mathbf{6}^-$, respectively. The maxima of absorption and extinction coefficients are compiled in Table 2 for the neutral materials and the one-electron reduction products of **1**−**4** and **6**.

Exhaustive electrolysis of solutions of **1** and **6** in acetonitrile required 1.89 C for 2.0×10^{-5} mol of **1** and 1.07 C for 1.15×10^{-5} mol of **6**. These values correspond to 0.98 ± 0.01 and 0.96 ± 0.01 Faradays mol^{-1} for reduction of **1** and **6**, respectively, and are consistent with a one-electron process. Reoxidation of the solutions of anion radical at 0.0 V (vs SCE) required 1.85 C for the solution of **1** and 1.04 C for the solution of **6**. These numbers correspond to 98% recovery of the neutral sulfone precursors from the anion radical. The reversibility of the reduction/oxidation cycle was confirmed by absorption spectroscopy. The absorption spectra of the reoxidized solutions were superimposable with those obtained before electrolysis and indicate that the radical anions of **1**, **3**, **4**, and **6** are stable over the experimental time frame of approximately 20 min. However, the reduction of the parent sulfone **2** was irreversible.

The high reversibility of the one-electron redox process in **1**, **3**, **4**, and **6** suggests that each of the spectral bands evident in the spectra of the reduction products is associated with optical transitions of the corresponding anion radical. Some ion radicals, however, are known to undergo reversible dimerization reactions.[26−28] The anion radical of TCNQ, which has a molecular structure similar to that of the sulfones discussed here, has been shown to exist in a monomer/dimer equilibrium in aqueous solutions.[28,29] We explored the possibility of reversible dimerization for the anion radicals of **1** and **6** by examination of the absorption spectra as a function of temperature and concentration. Absorption spectra for acetonitrile solutions of anion radicals of **1** and **6** were found to be independent of concentration over the range of 1×10^{-5} M to 4×10^{-4} M and independent of temperature from 0 °C to 60 °C. No evidence supportive of either anion−anion or anion−neutral association complexes was obtained.

Lithium Naphthalenide (LiNaph) Reduction of Sulfones 1−6 and 9. The one-electron, chemical reductions of neutral sulfones **1**−**6** and **9** in acetonitrile and **1**−**6** in dichloromethane and tetrahydrofuran (THF) were accomplished with the addition of a 1 M THF solution of LiNaph. Absorption spectra of the one-electron reduction products prepared in this manner for **1**−**6** in either acetonitrile or dichloromethane were identical to those produced via electrochemical reduction in these solvents.

Reduction of **9** either electrochemically or with LiNaph gave a relatively short-lived anion radical although the reduction is quasireversible by cyclic voltammetry. The anion radical of **9** was not observed spectroscopically at

(26) Lenhard, J. R.; Parton, R. L. *J. Am. Chem. Soc.* **1987**, *109*, 5808.
(27) Detty, M. R.; Haley, N. F.; Eachus, R. S.; Hassett, J. W.; Luss, H. R.; Mason, M. G.; McKelvey, J. M.; Wernberg, A. A. *J. Am. Chem. Soc.* **1985**, *107*, 6298.
(28) Boyd, R. H.; Phillips, W. O. *J. Chem. Phys.* **1965**, *43*, 2927.
(29) It should be noted that the dimerization equilibrium for TCNQ does not exist in nonaqueous solutions.

Table 2. Absorption Maxima for Neutral Sulfones 1–4 and 6 and Their One-Electron Reduction Products in Acetonitrile

	neutral sulfone		
compd	λ_{max}, nm	log ϵ	reduced species: λ_{max}, nm (log ϵ)[a]
1	371	4.45	603 (sh, 4.15), 556 (4.25), 303 (4.29)
2	309	4.38	615 (2.6), 460 (3.0), 295 (3.85), 235 (3.88)
3	319	4.44	550 (3.99), 506 (3.96), 366 (4.04), 320 (4.04)
4	333	4.43	560 (sh, 4.20), 528 (4.28), 307 (4.17)
6	420	4.44	612 (4.13), 595 (sh, 4.11), 510 (3.99), 436 (4.09), 318 (4.19)

[a] Starting with 5×10^{-4} M solution of neutral sulfone. Values in parentheses are values of log ϵ for the absorption bands assuming complete reduction to monomeric species.

Table 3. Lifetimes of Sulfone Anion Radicals in Solution at 295.0 ± 0.5 K As Determined Spectrophotometrically

	acetonitrile		tetrahydrofuran		dichloromethane	
neutral sulfone	k,[a] s^{-1}	$t_{1/2}$, min	k, s^{-1}	$t_{1/2}$, min	k,[a] s^{-1}	$t_{1/2}$, min
1	1.4×10^{-5}	825	5.8×10^{-4}	20	–	–
3	2.4×10^{-5}	480	1.2×10^{-3}	10	2.3×10^{-4}	50
4	6.6×10^{-6}	1750	3.9×10^{-4}	30	1.0×10^{-4}	115
6	9.3×10^{-6}	1240	1.2×10^{-4}	96	–	–
9	$>2 \times 10^{-2}$	≤0.5	–	–	–	–

[a] Rate constant for first-order loss of anion radical.

ambient temperature in dichloromethane. In acetonitrile, a magenta color formed but faded completely within minutes.

Lifetimes of Sulfone Anion Radicals in Solution. Anion-radical lifetimes in various solvents were calculated from the time-dependent changes in absorption spectra. Two modes of anion radical loss are possible: oxygen-assisted reoxidation to the neutral sulfone and irreversible decomposition to a stable product(s). In acetonitrile dried over molecular sieves, the rates of disappearance of the reduced species were identical for both electrochemical reduction of neutral sulfones in the presence of 0.1 M $TBABF_4$ and for reduction with LiNaph where no supporting electrolyte was present. The loss of anion radical appeared to follow first-order kinetics over the concentration range of 1×10^{-5} M to 1×10^{-4} M. As indicated from the data of Table 3, lifetimes in acetonitrile are 1–2 orders-of-magnitude larger than in either dichloromethane or THF.

Acetonitrile solutions of reduced sulfone were somewhat stable to air. The purple solutions of **1**, **4**, and **6** maintain their color for several days in vessels open to the air at 22 °C. Sulfone anion radicals were more sensitive to the air when dissolved in either dichloromethane or THF.

Other experiments indicate that the anion radicals are sensitive to the presence of water. The deliberate addition of water to a solution of the anion radical of **1** results in rapid loss of the spectral bands associated with the anion radical and appearance of bands associated with the neutral sulfone and a hydrolysis product with an absorption maximum at 648 nm. The anion radical of **6** was also reactive toward water but somewhat less so than **1**. The identities of the reaction products have not been determined. For all the sulfone anion radicals of this study, decomposition rates were greatly accelerated by the presence of aqueous base or acid.

EPR Spectra of Sulfone Anion Radicals. The sulfone anion radicals of **1** and **3–6** have sufficiently long lifetimes for EPR spectroscopic studies. The samples were prepared by electrochemical reduction of the neutral sulfones in acetonitrile or by the addition of LiNaph to acetonitrile or THF solutions of the neutral sulfones. The samples gave strong EPR signals (as illustrated in Figures 9 and 10 for $\mathbf{4}^-$ and $\mathbf{5}^-$, respectively, and in Figures 19–21 of the supplementary material for $\mathbf{1}^-$, $\mathbf{3}^-$, and $\mathbf{6}^-$) with resolved hyperfine structure. No paramagnetic signals were detected from acetonitrile or THF solutions of the reduction products of **2** and **9**.

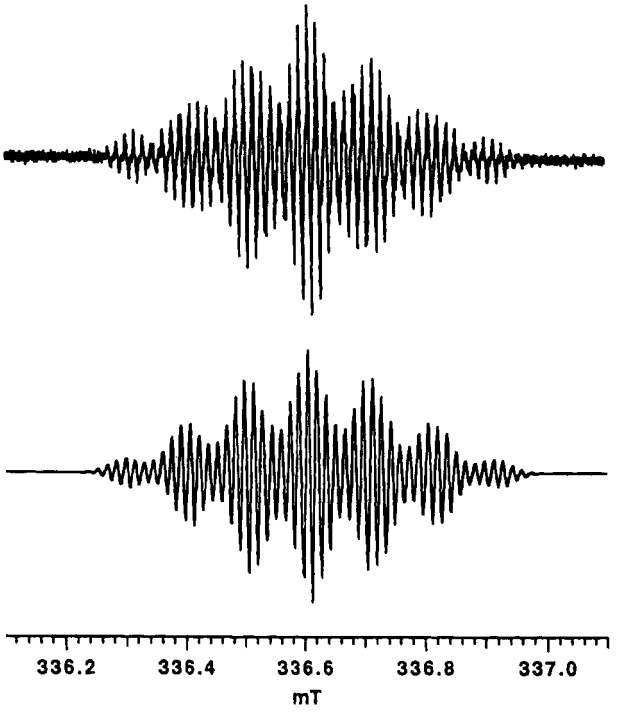

Figure 9. Experimental (top) and simulated (bottom) EPR spectra of the anion radical of **4** using the splitting parameters of Table 5.

The EPR spectra of the anion radicals of **1** and **3–6** were centered around g values of slightly greater than 2.000 (Table 4). Fitting the experimental spectra to calculated spectra (Figures 9 and 10) allowed the analysis of splitting constants a_N and a_H as compiled in Table 4. The EPR spectra were all characterized by a large nitrogen splitting of 1.0–1.5 mT and smaller splittings of 0.30–0.93 mT for the hydrogens at the 3- and 5-positions. Splittings from protons attached to the substituents at the 2- and 6-positions varied by more than 1 order of magnitude with the smallest values coming from the phenyl substituent in $\mathbf{4}^-$ and the largest value coming

Table 4. EPR Data for Anion Radicals of Sulfones 1 and 3–6

neutral sulfone	g	a_N, mT	$a_{H3,5}$, mT	R_1	a_{R1}, mT	R_2	a_{R2}, mT
1	2.0021	1.46	0.56	Ph	0.34 (6 H) ≤0.05 (4 H)	Ph	–
3	2.0021	1.42	0.487	*tert*-Bu	0.168 (18 H)	*tert*-Bu	–
4	2.0049	1.07	0.93	*tert*-Bu	0.155 (9 H)	Ph	0.145 (3 H), 0.025 (2 H)
5	2.0022	1.407	0.30	Ph	0.30 (3 H)	2-thienyl	1.52 (1 H) 1.38 (1 H)
6	2.0056	1.05[a]	0.32	2-thienyl	1.32[a] (4 H)	2-thienyl	–

[a] Interchangeable values (see text).

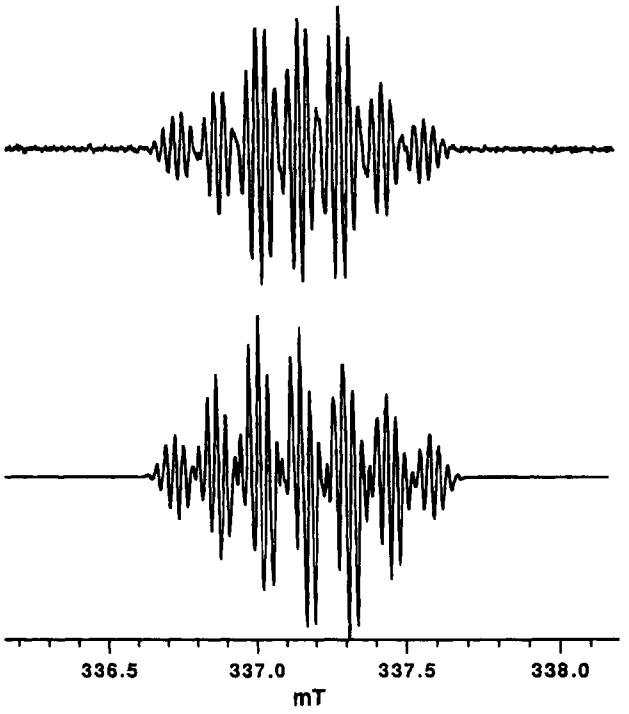

Figure 10. Experimental (top) and simulated (bottom) EPR spectra of the anion radical of **5** using the splitting parameters of Table 5.

from the 2-thienyl substituent in $\mathbf{5}^-$. For $\mathbf{6}^-$, the values of a_N and a_H for the four 2-thienyl protons are interchangeable since multiplicities would be very similar and the poor resolution of the experimental spectrum does not allow an unequivocal assignment. ENDOR spectroscopy would allow the unambiguous assignment of a values in these systems.[30] We have assumed symmetry in values of $a_{H3,5}$ for unsymmetrical sulfones $\mathbf{4}^-$ and $\mathbf{5}^-$, which need not be true. Again, ENDOR spectroscopy would allow the unambiguous assignment of values of a_H. Some asymmetry is apparent in the experimental EPR spectra of the anion radicals of **1** and **5** (Figure 10), which may be due to ion pairing.

One way of measuring substituent effects in these systems is by examination of the percentage of spin density at each substituent. The total a-value for protons attached to a carbon bearing unpaired spin is roughly 22.5 mT for a single π electron.[31] Thus, summing the a-values for the carbon atoms of each substituent and dividing by 22.5 should give an approximation of the spin densities for phenyl and 2-thienyl substituents. The percentages of spin density at the different substituents are summarized in Table 5.

(30) Eachus, R. S.; Olm, M. T. *Science* **1985**, *230*, 268.
(31) Carrington, A.; McLachlan, A. D. *Introduction to Magnetic Resonance*; Chapman and Hall: London, 1967.

Table 5. Percentage of Unpaired Spin Found at Different Sites in Anion Radicals of Sulfones 1 and 3–6

neutral sulfone	$H_{3,5}$, % spin	R_1	% spin	R_2	% spin
1	4.9	Ph	4.8	Ph	4.8
3	4.2	*tert*-Bu	6.6	*tert*-Bu	6.6
4	8.1	*tert*-Bu	6.1	Ph	2.1
5	2.6	Ph	3.9	2-thienyl	13.9
6	2.8	2-thienyl	11.5 (9.1)[a]	2-thienyl	11.5 (9.1)[a]

[a] For two possible values of a_H (see text).

The *tert*-butyl substituents interact with the unpaired spin via a hyperconjugation mechanism, which might affect the spin densities at the atoms of the π-framework. If the hyperconjugation of the unpaired spin in the *tert*-butyl group is approximated by a series of methyl-radical-like contributions to a carbon orbital aligned with the π-framework, then the maximum possible contribution from the *tert*-butyl group would be that of a methyl radical, which is a total splitting of 22.7 mT.[32] Based on the 22.7-mT number, the sum of all eighteen *tert*-butyl protons in the anion radical of **3** is indicative of approximately 7% of a methyl radical from hyperconjugation in each *tert*-butyl group. In unsymmetrical $\mathbf{4}^-$ bearing one phenyl substituent and one *tert*-butyl substituent, approximately 6% of a methyl radical is found in the anion radical from hyperconjugation of the *tert*-butyl group.

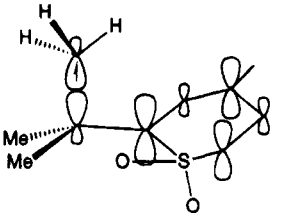

Experimental values of electron density at nitrogen, ϱ^N, cannot be determined unambiguously from a_N for the sulfones of this study since both s- and p-orbital contributions are not known. However, the values of a_N in the sulfones of this study (1.05–1.46 mT) are quite similar to those obtained for TCNQ (0.99 mT)[6] and its cyanoimine-containing derivatives (1.21 mT[16] and 1.10 mT[17]). If one assumes that the simple relationship $a_N = Q_1^N \varrho^N$ holds,[33] where Q_1^N is about 20 mT and ϱ^N is the unpaired electron density at nitrogen, then ϱ^N in the anion radicals **1** and **3**–**6** would be 4–6% of the total spin.

***Ab Initio* Calculations on the Anion Radical of 9.** The anion radical of **9**, which experimentally is of too short a lifetime for EPR studies in our experimental

(32) Reference 30, p 84.
(33) Carrington, A.; does Santos-Veiga, J. *Mol. Phys.* **1962**, *5*, 21. (b) Gordy, W. *Theory and Application of Electron Spin Resonance, Techniques of Chemistry Vol. XV*; West, W., Ed.; Wiley-Interscience: New York, 1980; p 250.

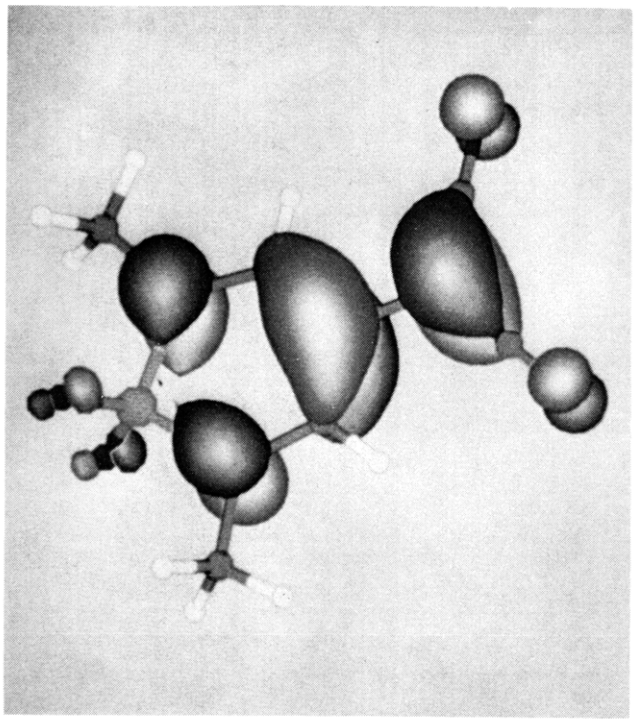

Figure 11. An isosurface of the SOMO of the anion-radical of **9** as determined by an *ab initio* calculation. The graphic was produced by The Chemistry Viewer, Molecular Simulations, Inc., Burlington, MA.

Table 6. Atom Spin Densities in the Anion Radical of 9 As Calculated for Full Geometry Optimization with Restricted Open-Shell Hartree–Fock with 6-31G* Basis

atom	atomic spin density	atom	atomic spin density
S	0.027	C_7	0.209
O	0.008	C_8	0.016
C_2	0.108	C_9	0.016
C_3	0.033	N_1	0.042
C_4	0.335	N_2	0.042
C_5	0.033	C_{10}	0.000
C_6	0.108	C_{11}	0.000
H_1	0.000	H_3	0.000
H_2	0.000		

setup, was examined by *ab initio* methods[34] with full geometry optimization with restricted open-shell Hartree–Fock and 6-31G* basis. The numbering scheme is shown below. An isosurface of the SOMO of the anion radical is shown in Figure 11 and atomic spin densities are compiled in Table 6. The largest spin densities are found at C_2, C_4, C_6, and C_7. Little spin density is calculated for the methyl substituents of **9**.

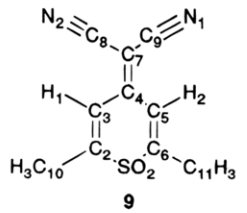

9

The *ab initio*-computed values of free spin at the various atoms in the anion radical of **9** are in excellent agreement with the experimental observations for anion radicals of **1** and **3**–**6**. The 6-31G* calculation suggests that approximately 4.2% of the spin is found at each nitrogen in **9**, which supports the assumption that contributions to a_N are primarily from the unpaired spin in the p-orbital. Experimental values of a_H suggest that 1.4–4.0% of the free spin is found at both C_3 and C_5 in the anion radicals of this study. These data are in good agreement with the 6-31G* calculation for **9** in which C_3 and C_5 are each predicted to bear 3.3% of the free spin. The bulk of the spin density is predicted by the 6-31G* calculation to be at C4 and C7 in the anion radical of **9**, which are unobservable sites by EPR.

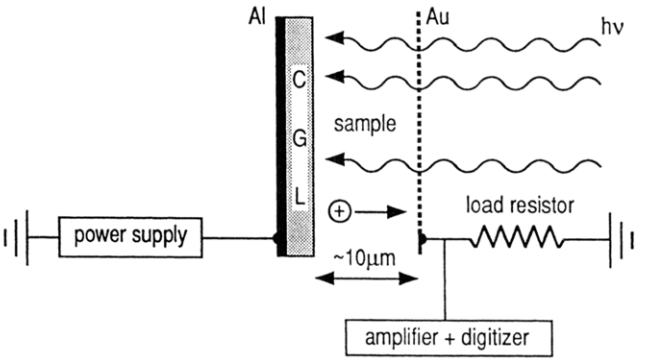

Figure 12. A typical time-of-flight experiment. The sample, a thin film consisting of the 1,1-dioxothiopyran (electron-transport material) molecularly dispersed in a polymeric binder, is sandwiched between (a) a submicron charge-generation layer (CGL) and Al/SiO_2 electrode and (b) a semitransparent Au electrode. The Au layer is connected to a high-voltage power supply. The Al electrode is connected to ground through a current-sensing resistor. A flash of light generates electron-hole pairs in the CGL. The electrons are drawn into and through the sample by the applied electric field. Their motion induces a "photo" current through the external circuit and a proportional potential drop across the resistor. The latter is amplified and recorded. The photocurrent is proportional to the number and average velocity of the electrons drifting through the film.

Electron Mobilities Measured in Thin Films of Sulfones 3, 4, and 15 in a Polymer Matrix. While compounds **1**, **5**, and **6** of this study were too sparingly soluble for the concentrations required to make usable thin films for a CTL, compounds **15** (which is structurally quite similar to **1**), **3**, and **4** were sufficiently soluble for coating from dichloromethane at a total solids concentration of 10% by weight (approximately 15% **3**, **4**, or **15**; 85% polymer). Electron mobilities were measured by the standard time-of-flight experiment, as illustrated in Figure 12.[1b] The CGL was a 0.5-μm-thick layer of a microcrystalline tetrafluorophthalocyanine finely dispersed in a polyester binder.[20b,35] The CTL consisted of sulfone **15**, **3**, or **4** molecularly dispersed in a polyester binder coated over the CGL, typically 10-μm-thick. The capacitance across the film was used to evaluate the thickness of the sample, assuming a dielectric constant of **3** and neglecting the thickness of the CGL.

In the time-of-flight experiment, one electrode (*e.g.* the aluminum layer in Figure 12) is connected to a high-voltage power supply and the other (gold) electrode is connected to ground through a current-sensing resistor. Flash illumination generates electron-hole pairs in the

(34) *Gaussian 92*, Revision A: Frisch, M. J.; Trucks, G. W.; Head-Gordon, M.; Gill, P. M. W.; Wong, M. W.; Foresman, J. B.; Johnson, B. G.; Schlegel, H. B.; Robb, M. A.; Replogie, E. S.; Gomperts, R.; Andres, J. L.; Raghavachari, K.; Binkley, J. S.; Gonzalez, C.; Martin, R. L.; Fox, D. J.; Defrees, D. J.; Baker, J.; Stewart, J. J. P.; Pople, J. A., Gaussian, Inc., Pittsburgh, PA, 1992.

(35) Hung, Y.; Klose, T. R.; Regan, M. T.; Rossi, L. J. U.S. Patent 4,701,396 (1986).

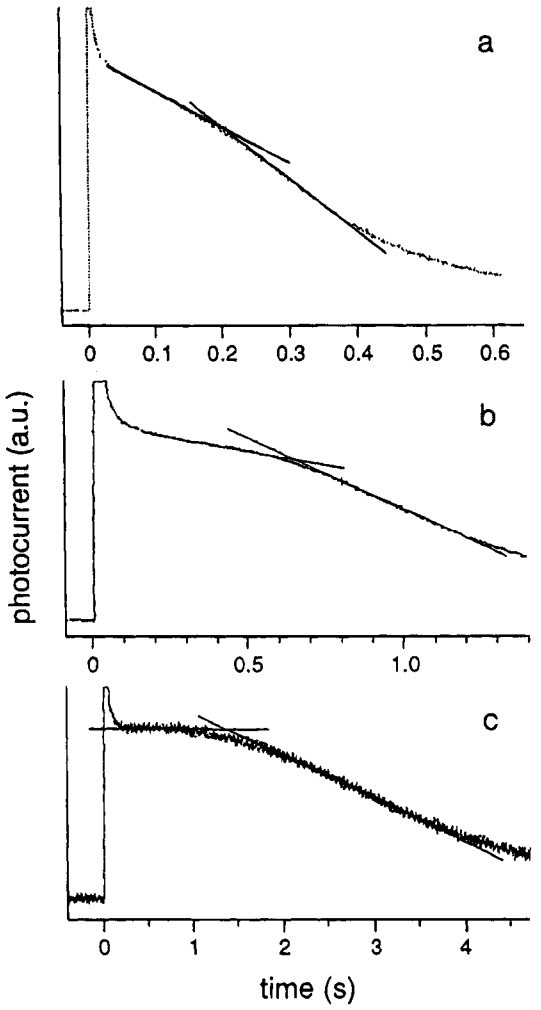

Figure 13. Typical photocurrent transients for (a) **15**, (b) **4**, and (c) **3**. The transit time was determined by the crossing of tangents to the early "plateau" and the late "tail".

CGL. The electrons are drawn into and through the sample by the applied electric field (E). Their motion induces a current through the external circuit and a proportional potential drop across the resistor. Ideally, the current would be constant until the electrons reach the gold surface and then fall to zero. The transit time, thus defined, together with the thickness of the sample gives the velocity (v) and the mobility (μ) is set equal to v/E.

In nonideal systems, the current trace is characterized by an initial spike, a plateau, and a tail, as shown in Figure 13. The transit time is determined, somewhat arbitrarily,[1b] by drawing tangents to the plateau and to the steepest part of the tail, and taking the transit time as their intersection. In Figure 14, the electron mobilities at room temperature are plotted against electric field strength and show the trend μ(**15**) > μ(**4**) > μ(**3**), irrespective of field strength.

1,1-Dioxothiopyrans **5** and **6** were sparingly soluble in coating solvents and molecularly dispersed polymeric films containing these materials were prone to crystallization, which render them unsuitable for mobility measurements. However, initial studies with **16** show electron mobility that is a factor of three greater in molecularly dispersed polymeric films containing **16** at 30% by weight relative to films containing **15** at 30% by weight.

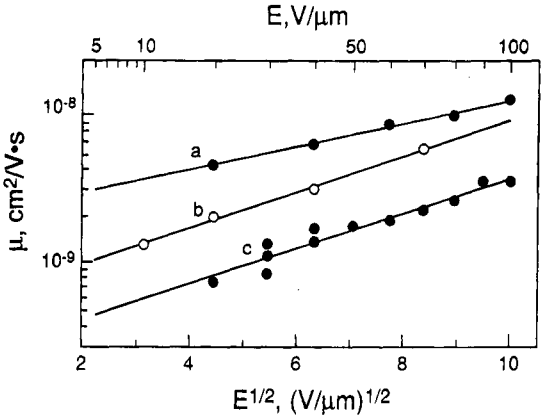

Figure 14. Electron mobility at room temperature plotted vs electric field strength (E) for (a) **15**, (b) **4**, and (c) **3**. Weight fractions (17.4, 15.8, and 14.8%, respectively) are adjusted so that molar concentrations of electron-transport materials are equal. The horizontal axis is linear in $E^{1/2}$ because this choice usually gives linear semilogarithmic plots.[1b,39]

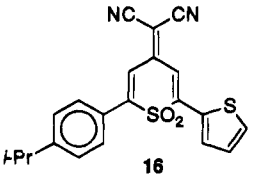

16

Summary and Conclusions

In the Bässler formalism,[9] site energies and intersite distances are important parameters in determining electron mobilities in molecularly dispersed polymers. Differences in reduction potentials for electron transport materials are in part responsible for the differences in site energies. The differences in reduction potentials of 1,1-dioxothiopyrans **1**–**15** of this study are only 0.223 V for the introduction of one electron. Among **3**, **4**, **15**, and **16**, the differences in reduction potentials to generate the corresponding anions are only 0.175 V (≈4 kcal mol^{-1}) while mobilities in polymer binders containing these materials vary by more than 1 order of magnitude. The differences in reduction potentials seem relatively small to explain differences observed in electron mobilities, μ.

Changes in intersite distances for electron hopping might also influence the mobility of electrons. Flatter molecules should permit closer stacking and decrease the intersite distance. Increased π-delocalization of the unpaired spin might serve as an antenna, which would increase overlap among adjacent sites and also decrease the intersite distance. The bulky *tert*-butyl groups disrupt the planarity of the thiopyran ring in **3** and **4** and also increase the minimum intermolecular distance between two transport molecules. The mobility of molecularly dispersed polymeric films containing the di-*tert*-butyl derivative **3** is a factor of 3 lower than those containing the more planar 2-phenyl-6-*tert*-butyl derivative **4**. In **4**, the phenyl group is sterically much smaller than the second *tert*-butyl group in **3** and also extends the π-conjugation of the anion radical of **4** relative to the anion radical of **3**. The 2,6-diphenyl derivative **1** is nearly planar and has two π-delocalizing phenyl substituents, and the mobility of molecularly dispersed polymeric films containing **15**, which is structurally and electronically similar to **1**, is 1 order of magnitude greater than the mobility of molecularly dispersed polymeric films containing **3**. The reduction potentials of 2-thienyl-substi-

tuted derivatives **5** (−0.185 V vs SCE), **6** (−0.171 V vs SCE), and **16** (−0.189 V vs SCE) are quite similar to those of **1** (−0.203 V vs SCE) and **15** (−0.219 V vs SCE). Energy differences among sites in molecularly dispersed polymers of these four systems should be minimal. The 2-thienyl substituents have much larger spin densities than the phenyl substituents in the corresponding anion radicals as determined by EPR spectroscopy, which suggests increased delocalization. In the crystal structure of **5**, the 2-thienyl substituent is rigorously coplanar with the thiopyran ring. Both the increased delocalization and the increased planarity should minimize intersite distances and increase mobility in systems containing the 2-thienyl substituent. The increased mobility of electrons in CTL's containing **16** relative to those containing **15** is supportive of the importance of both planarity and π-delocalization in electron transport materials.

Experimental Section

Melting points were determined on a Thomas-Hoover melting point apparatus and are uncorrected. ^{1}H NMR spectra were recorded either on a General Electric QE-300 spectrometer or on a Varian Gemini-200 spectrometer. UV-visible–near infrared spectra were recorded on a Perkin-Elmer Lambda 9 spectrophotometer. Infrared spectra were recorded on a Beckman IR 4250 instrument. Microanalyses were performed on a Perkin-Elmer 240 C, H, and N Analyzer. Tetrahydrofuran (THF) and CH_2Cl_2 were purchased as anhydrous from Aldrich Chemical Co. and were used as received. Acetonitrile (MCB spectrograde) was dried over 4A molecular sieves (Kodak Laboratory Chemicals, baked at 400 °C). Tetrabutylammonium tetrafluoroborate ($TBABF_4$, Kodak Laboratory Chemicals) was recrystallized three times from ethanol/water, vacuum dried at 50 °C, and stored in a desiccator. Compound **1** was prepared as previously described in ref 19.

Preparation of 4*H*-1,1-Dioxo-4-(dicyanomethylidene)-thiopyran (2). 1,1-Dioxo-4*H*-thiopyran-4-one (0.292 g, 2.00 mmol) and malononitrile (0.20 g, 3.0 mmol) were slurried in 20 mL of CH_2Cl_2. The reaction mixture was cooled to 0 °C and basic alumina (2.0 g) was added. The resulting slurry was stirred for 1 h at ambient temperature. The reaction mixture was filtered through Celite and the filter cake was washed with several portions of CH_2Cl_2. The combined filtrates were concentrated. The residue was recrystallized from ethyl acetate to give 0.083 g (22%) of cubic, white crystals, mp 184–188 °C (dec): ^{1}H NMR ($CDCl_3$) δ 7.315 (AA'BB', 2 H, J = 11.4 Hz for "doublet" splitting), 7.06 (AA'BB', 2 H, J = 11.4 Hz for "doublet" splitting); IR (KBr) 3035, 2130, 1307, 1300, 1185, 1119, 870, 796 cm^{-1}. Anal. Calcd for $C_8H_4N_2O_2S$: C, 49.99; H, 2.10; N, 14.58. Found: C, 50.07; H, 2.11; N, 14.51.

Preparation of 4*H*-1,1-Dioxo-2,6-di-*tert*-butyl-4-(dicyanomethylidene)thiopyran (3). A mixture of 4*H*-1,1-dioxo-2,6-di-*tert*-butylthiopyran-4-one (1.28 g, 5.0 mmol), malononitrile (0.66 g, 10 mmol), and basic alumina (2.02 g, 20.0 mmol) in 15 mL of CH_2Cl_2 were stirred 4 h at ambient temperature. The reaction mixture was filtered through a 10-g plug of silica gel eluted with CH_2Cl_2. The residue was recrystallized from 20 mL of 1:1 ethyl acetate/hexanes to give 0.91 g (60%) of **3** as a white crystalline solid, mp 145–146 °C: ^{1}H NMR ($CDCl_3$) δ 7.18 (s, 2 H), 1.55 (s, 18 H); ^{13}C NMR ($CDCl_3$) δ 149.7, 147.8, 123.7, 111.8, 89.0, 39.7, 31.1; IR (KBr) 2222, 1651, 1602 cm^{-1}; FDMS, m^+/z 304 ($C_{16}H_{20}N_2O_2S$). Anal. Calcd for $C_{16}H_{20}N_2O_2S$: C, 63.13; H, 6.62; N, 9.20. Found: C, 62.73; H, 6.54; N, 9.39.

Preparation of 4*H*-1,1-Dioxo-2-phenyl-6-*tert*-butyl-4-(dicyanomethylidene)thiopyran (4). A mixture of 5.20 g (0.0188 mol) of 4*H*-1,1-dioxo-2-phenyl-6-*tert*-butylthiopyran-4-one and 1.65 g (0.025 mol) of malononitrile in 20 mL of ethanol was heated at reflux with mechanical stirring. To this solution, 0.20 mL of piperidine in 5 mL of ethanol was added dropwise via pressure equalizing addition funnel. After 4 h at reflux, the reaction mixture was cooled to ambient temperature. The crystalline solid was collected by filtration and washed with 20 mL of ethanol. The solid was heated to boiling in ethyl acetate/ethanol, cooled, and filtered to give 4.20 g (69%) of a burnt-orange crystalline solid, mp 175–177 °C: ^{1}H NMR ($CDCl_3$) δ 7.79 (m, 2 H), 7.62–7.48 (m, 3 H), 7.20 (d, 1 H, J = 2.6 Hz), 7.18 (d, 1 H, J = 2.6 Hz), 1.55 (s, 9 H); ^{13}C NMR ($CDCl_3$) δ 161.3, 152.1, 148.7, 132.65, 129.8, 129.6, 129.4, 122.2, 122.1, 111.8, 89.1, 39.7, 31.1; IR (KBr) 2965, 2220, 1629, 1570, 1514, 1303, 1130, 886, 760 cm^{-1}; FDMS m/z 324 ($C_{18}H_{16}N_2O_2S$). Anal. Calcd for $C_{18}H_{16}N_2O_2S$: C, 66.65; H, 4.97; N, 8.64; S, 9.88. Found: C, 66.26; H, 4.99; N, 8.52; S, 9.40.

Preparation of 4*H*-1,1-Dioxo-2-phenyl-6-(2-thienyl)-4-(dicyanomethylidene)thiopyran (5). Prepared as described for **4**: 64% of a burnt-orange crystalline solid, mp 2227–232 °C: ^{1}H NMR ($CDCl_3$) δ 7.98 (d × d, 1 H, J = 1, 4 Hz), 7.82 (d × d, 2 H, J = 2, 8 Hz), 7.67 (d × d, 1 H, J = 1, 5 Hz), 7.54 (m, 3 H), 7.32 (d, 1 H, J = 2.7 Hz), 7.23 (d, 1 H, J = 2.7 Hz), 7.21 (d × d, 2 H, J = 4, 5 Hz); ^{13}C NMR (CD_2Cl_2) δ 167.4, 149.9, 148.2, 144.8, 134.2, 133.7, 132.95, 130.4, 130.2, 130.0, 129.6, 123.8, 119.2, 112.6, 112.5, 88.9; IR (KBr) 2225, 1315, 1140 cm^{-1}; FDMS, m^+/z 350 ($C_{18}H_{10}N_2O_2S_2$). Anal. Calcd for $C_{18}H_{10}N_2O_2S_2$: C, 61.70; H, 2.88; N, 7.99; S, 18.30. Found: C, 61.28; H, 2.97; N, 7.93; S, 18.27.

Preparation of 4*H*-1,1-Dioxo-2,6-di-(2-thienyl)-4-(dicyanomethylidene)thiopyran (6). Prepared as described for **4**: 73% of a burnt-orange crystalline solid, mp 259–263 °C: ^{1}H NMR ($CDCl_3$) δ 7.98 (d, 2 H, J = 4 Hz), 7.68 (d, 2 H, J = 5 Hz), 7.24 (d × d, 2 H, J = 4, 5 Hz), 7.30 (s, 2 H); ^{13}C NMR (CD_2Cl_2, sparingly soluble) δ 167.3, 133.9, 133.6, 130.35, 121.8, 120.0, 119.5, 88.2; IR (KBr) 3140, 2220, 1612, 1550, 1315 cm^{-1}; FDMS, m/z 356 ($C_{16}H_8N_2O_2S_3$). Anal. Calcd for $C_{16}H_8N_2O_2S_3$: C, 53.92; H, 2.26; N, 7.86; S, 26.99. Found: C, 53.59; H, 2.40; N, 7.70; S, 26.91.

Preparation of 4*H*-1,1-Dioxo-2,6-di-(3-thienyl)-4-(dicyanomethylidene)thiopyran (7). Prepared as described for **4**: 83% of a burnt-orange crystalline solid, mp 275–285 °C: ^{1}H NMR ($CDCl_3$) δ 8.27 (t, 2 H, J = 2 Hz), 7.52 (d, 4 H, J = 2 Hz), 7.35 (s, 2 H); IR (KBr) 3140, 2225, 1615, 1560, 1490, 1310, 1135, 795 cm^{-1}; FDMS, m/z 356 ($C_{16}H_8N_2O_2S_3$). Anal. Calcd for $C_{16}H_8N_2O_2S_3$: C, 53.92; H, 2.26; N, 7.86; S, 26.99. Found: C, 54.08; H, 2.38; N, 8.01; S, 26.14.

Preparation of 4*H*-1,1-Dioxo-2,6-di-(2-furanyl)-4-(dicyanomethylidene)thiopyran (8). Prepared as described for **4**: 49% of a burnt-orange crystalline solid, mp 295–296 °C: ^{1}H NMR ($CDCl_3$) δ 8.27 (t, 2 H, J = 2 Hz), 7.52 (d, 4 H, J = 2 Hz), 7.35 (s, 2 H); IR (KBr) 3160, 2225, 1615, 1545, 1360, 1340, 1145, 1035, 770 cm^{-1}; FDMS, m/z 324 ($C_{16}H_8N_2O_2S$). Anal. Calcd for $C_{16}H_8N_2O_4S$: C, 59.26; H, 2.49; N, 8.64. Found: C, 59.08; H, 2.65; N, 8.43.

Preparation of 4*H*-1,1-Dioxo-2,6-dimethyl-4-(dicyanomethylidene)thiopyran (9). Prepared as described for **3**: 43% of a white crystalline solid, mp 173–176 °C: ^{1}H NMR ($CDCl_3$) δ 7.00 (s, 2 H), 2.45 (s, 6 H); ^{13}C NMR ($CDCl_3$) δ 149.7, 147.8, 123.7, 111.6, 88.6, 15.2; IR (KBr) 2222, 1651, 1602, 1529, 1447, 1311, 1303 (sh), 1160, 1118 cm^{-1}; FDMS, m^+/z 220 ($C_{10}H_8N_2O_2S$). Anal. Calcd for $C_{10}H_8N_2O_2S$: C, 54.53; H, 3.66; N, 12.72. Found: C, 54.73; H, 3.54; N, 12.80.

4*H*-1,1-Dioxo-2-phenyl-6-methyl-4-(dicyanomethylidene)thiopyran (10). Prepared as described for **4**: 67%, mp 165–167 °C; ^{1}H NMR ($CDCl_3$) δ 7.82 (m, 2 H), 7.65–7.45 (m, 3 H), 7.27 (d, 1 H, J = 3.0 Hz), 7.06 (m, 1 H), 2.50 (d, 3 H, J = 1.2 Hz); IR (KBr) 2220, 1568, 1305, 1143, 1117 cm^{-1}; FDMS, m/z 282 ($C_{15}H_{10}N_2O_2S$). Anal. Calcd for $C_{15}H_{10}N_2O_2S$: C, 63.81; H, 3.57; N, 9.92. Found: C, 63.65; H, 3.56; N, 9.89.

4*H*-1,1-Dioxo-2-(2-thienyl)-6-*tert*-butyl-4-(dicyanomethylidene)thiopyran (11). Prepared as described for **4**: 30%, 163.5–165 °C; ^{1}H NMR ($CDCl_3$) δ 7.97 (d, 1 H, J = 3.8 Hz), 7.68 (d, 1 H, J = 5.1 Hz), 7.25 (d, 1 H, J = 2.6 Hz), 7.23 (m, 2 H), 7.16 (d, 1 H, J = 2.6 Hz), 1.56 (s, 9 H); IR (KBr) 2215, 1620, 1564, 1303, 1132 cm^{-1}; FDMS, m^+/z 330 ($C_{16}H_{14}N_2O_2S_2$). Anal. Calcd for $C_{16}H_{14}N_2O_2S_2$: C, 58.14; H, 4.27; N, 8.48. Found: C, 57.96; H, 4.31; N, 8.55.

Preparation of 4*H*-1,1-Dioxo-2-phenyl-6-(3-thienyl)-4-(dicyanomethylidene)thiopyran (12). Prepared as described for **4**: 79% of a burnt-orange crystalline solid, mp 223–228 °C: ^{1}H NMR ($CDCl_3$) δ 8.27 (t, 1 H, J = 1 Hz), 7.84 (d × d, 2 H, J = 2, 8 Hz), 7.4–7.7 (m, 5 H), 7.54 (m, 5 H), 7.36 (d, 1 H, J = 2.7 Hz), 7.28 (d, 1 H, J = 2.7 Hz); ^{13}C NMR (CD_2Cl_2, sparingly soluble) δ 150.1, 148.7, 145.3, 133.0, 131.9, 130.2, 129.9, 129.75, 129.70, 128.8, 127.0, 123.65, 120.5; IR (KBr) 2225, 1625, 1565, 1310, 1135 cm^{-1}; FDMS, m^+/z 350 ($C_{18}H_{10}N_2O_2S_2$). Anal. Calcd for $C_{18}H_{10}N_2O_2S_2$: C, 61.70; H, 2.88; N, 7.99; S, 18.30. Found: C, 61.61; H, 2.98; N, 7.92; S, 18.00.

Preparation of 4*H*-1,1-Dioxo-2-phenyl-6-(2-furanyl)-4-(dicyanomethylidene)thiopyran (13). Prepared as described for **4**: 65% of a burnt-orange crystalline solid, mp 226.5–230 °C: ^{1}H NMR ($CDCl_3$) δ 7.81 (m, 2 H), 7.73 (d, 1 H, J = 1.8 Hz), 7.54 (m, 3 H), 7.44 (d, 1 H, J = 3.6 Hz), 7.26 (d, 1 H, J = 2.4 Hz), 7.23 (d, 1 H, J = 2.4 Hz), 6.68 (d × d, 1 H, J = 1.8, 3.6 Hz); ^{13}C NMR (CD_2Cl_2, sparingly soluble) δ 149.3, 149.0, 148.0, 144.2, 139.8, 132.9, 130.2, 129.95, 129.4, 124.15, 120.4, 116.5, 115.1, 112.7, 88.6; IR (KBr) 2225, 1315, 1140, 765 cm^{-1}; FDMS, m^+/z 334 ($C_{18}H_{10}N_2O_3S$). Anal. Calcd for $C_{18}H_{10}N_2O_3S$: C, 64.66; H, 3.01; N, 8.38; S, 9.59. Found: C, 64.51; H, 3.03; N, 8.26; S, 9.30.

4*H*-1,1-Dioxo-2-phenyl-6-(*n*-butyl)-4-(dicyanomethylidene)thiopyran (14). Prepared as described for **4**: 29%, mp 132.5–133 °C; ^{1}H NMR ($CDCl_3$) δ 7.82 (m, 2 H), 7.65–7.45 (m, 3 H), 7.26 (d, 1 H, J = 1.0 Hz), 7.02 (d, 1 H, J = 1 Hz), 2.81 (br t, 2 H, J = 7.9 Hz), 1.77 (m, 2 H), 1.50 (m, 2 H), 1.00 (t, 3 H, J = 7.3 Hz); ^{13}C NMR ($CDCl_3$) δ 154.4, 150.5, 148.2, 132.8, 129.95, 129.4, 122.7, 122.1, 111.8, 89.0, 30.5, 28.4, 22.8, 14.2; IR (KBr) 2965, 2220, 1640 cm^{-1}; FDMS, m/z 324 ($C_{18}H_{16}N_2O_2S$). Anal. Calcd for $C_{15}H_{10}N_2O_2S$: C, 66.65; H, 4.97; N, 8.64; S, 9.88. Found: C, 66.49; H, 5.00; N, 8.53; S, 9.14.

Preparation of 4*H*-1,1-Dioxo-2-(*p*-tolyl)-6-phenyl-4-(dicyanomethylidene)thiopyran (15). Prepared as described for **4**: 80% of a burnt-orange crystalline solid, mp 181–183 °C; ^{1}H NMR ($CDCl_3$) δ 7.87 (m, 2 H), 7.79 (d, 2 H, J = 8.6 Hz), 7.60 (m, 3 H), 7.37 (d, 2 H, J = 8.6 Hz), 7.33 (s, 2 H), 2.45 (s, 3 H); ^{13}C NMR (CD_2Cl_2, sparingly soluble) δ 150.5, 148.7, 144.3, 132.95, 131.0, 130.2, 129.93, 129.86, 129.7, 126.9, 123.5, 122.4, 112.4, 89.9, 22.2; IR (KBr) 2230, 1313, 1139 cm^{-1}; FDMS, m/z 358 ($C_{21}H_{14}N_2O_2S$). Anal. Calcd for $C_{21}H_{14}N_2O_2S$: C, 70.37; H, 3.94; N, 7.82. Found: C, 70.59; H, 3.80; N, 7.70.

Preparation of 4*H*-1,1-Dioxo-2-(4-isopropylphenyl)-6-(2-thienyl)-4-(dicyanomethylidene)thiopyran (16). Prepared as described for **4**: 55% of a burnt-orange crystalline solid, mp 199–201 °C; ^{1}H NMR ($CDCl_3$) δ 7.99 (d × d, 1 H, J = 1, 4 Hz), 7.78 (AA′BB′, 2 H), 7.67 (d × d, 1 H, J = 1, 5 Hz), 7.37 (AA′BB′, 2 H), 7.32 (d, 1 H, J = 2.6 Hz), 7.26 (d, 1 H, J = 2.6 Hz), 7.225 (d × d, 2 H, J = 4, 5 Hz), 2.97 (septet, 1 H), 1.27 (d, 6 H); IR (KBr) 2225, 1305, 1135 cm^{-1}; FDMS, m^+/z 392 ($C_{21}H_{16}N_2O_2S_2$). Anal. Calcd for $C_{21}H_{16}N_2O_2S_2$: C, 64.26; H, 4.11; N, 7.14. Found: C, 64.26; H, 4.16; N, 7.19.

Electrochemistry. Voltammetry experiments were performed using a Princeton Applied Research Corp. (PAR) 173 potentiostat in conjunction with PAR Model 175 universal programmer and PAR Model 179 digital coulometer and a 14A Lock-in amplifier. A Hewlett-Packard Model 239A low-distortion oscillator was used in AC measurements. Solutions for voltammetric examination contained 0.1 M $TBABF_4$ in acetonitrile and ca. 5 × 10^{-4} M sulfone and were deaerated with argon prior to examination. Working electrodes were Pt disk (Bioanalytical Systems) and were polished with 1-μm diamond paste (Buhler Metadi), rinsed with water, and dried before each experiment. All potentials were measured at 22 °C vs the NaCl saturated calomel electrode (SSCE). A two-compartment, three-electrode voltammetry cell was utilized. Contact between the SSCE and nonaqueous electrolyte was accompanied using a porous Vycor disk. Relative to this SSCE the $E^{O\prime}$ for ferrocene was measured to be 0.417 V. Reduction potentials were measured by phase selective second-harmonic AC voltammetry as described previously.[23]

UV-Vis Spectroscopy. Solutions of sulfone anion radical were prepared by chemical or coulometric methods. Chemical reductions were performed using a slight excess of lithium naphthalenide (LiNaph) in THF with ca. 5 × 10^{-4} M solutions of sulfone. Electrolysis was accomplished via controlled-potential coulometry with a PAR Model 337A (three compartment) coulometric cell system equipped with a 67-cm^2 area Pt gauze working electrode (electrolysis time for >98% reduction is ca. 2 min). In a few experiments, a tubular electrochemical flow cell was used that was of a design similar to that of Miner and Kissinger[36] except that the working electrode was compressed Pt gauze (Fisher). Electrolysis times of ca. 10 s could be achieved using the flow-cell system. In all electrolysis experiments, the working electrode was poised at a potential 200 mV beyond the reversible reduction potential of the sulfone. The electrolyzed solutions were rapidly pumped through 0.8-mm inner-diameter Teflon tubing to a 1-mm or 10-mm quartz spectral flow cell (Helma) for absorption measurement. Spectra and kinetic measurements were performed under conditions of no-flow. Spectra were obtained with a Hewlett-Packard 8450A diode array spectrophotometer.

Preparation of Lithium Naphthalenide (LiNaph). Lithium wire (0.45 g, 0.065 mol) was cut into 0.5-cm pieces under oil. The resulting pieces were washed with heptane, dried under argon, and added to a stirred solution of 9.52 g (0.0743 mol) of naphthalene in 60 mL of anhydrous THF. The resulting solution was stirred overnight under argon giving a dark green solution. Syringe-transfer of the 1.0 M solution was employed in reductions using the reagent.

Preparation of EPR Samples. Method A. A 1.00 × 10^{-4} mol sample of sulfone was dissolved in 50.0 mL of anhydrous, degassed THF to give 2.0 × 10^{-3} M solutions of the sulfone. To these solutions was added 0.10 mL of the lithium naphthalenide solution to give a 2 × 10^{-3} M solution of the anion radical. A 0.5-mL aliquot of the resulting solution was transferred under argon via a gas-tight syringe into a 5-mm quartz EPR tube. The sample tube was then degassed via repeated freeze-pump-thaw cycles to remove oxygen.

Method B. The procedure of method A was repeated except that anhydrous acetonitrile was employed as solvent.

Method C. The bulk electrolysis samples in acetonitrile with 0.1 M $TBABF_4$ were collected directly in a 5-mm quartz tube. The sample tube was then degassed via repeated freeze-pump-thaw cycles to remove oxygen.

EPR Spectra. EPR spectra were recorded and simulated to second order with a Bruker ESP 300E EPR spectrometer operating at 9.44 GHz and room temperature.

X-ray Crystal Structures of Sulfones 1–5. Data were collected on an Enraf-Nonius CAD4 diffractometer using graphite monochromated Mo Kα (**1**, **3**–**5**) and Cu Kα (**2**) radiation at 293 ± 1 K. The structures were solved by direct methods (MULTAN80[37] for **1**, **3**, and **4** and SHELXS[38] for **2** and **5**) and refined by the full-matrix least-squares method. Hydrogen atoms were found in a difference electron density map and were included in the refinement. Programs used in this study were from: MolEN, An Interactive Structure Solution Procedure, Enraf-Nonius, Delft, The Netherlands (1990) and SHELXTL v.4.1, Siemens Analytical X-Ray Instruments, Inc., Madison, WI (1990). Crystal data is contained in Table 7.[39]

Preparation of Samples for Measurement of Electron Mobility. An aluminized poly(ethylene terephthalate) substrate was overcoated with a 500-Å-thick insulating layer of SiO_2 and a 0.5-μm-thick CGL of a microcrystalline tetrafluorophthalocyanine finely dispersed in a polyester binder.[20b,35]

(36) Miner, D. J.; Kissinger, P. T. *Biochem. Pharmacol.* **1979**, *28*, 3285.

(37) Main, P.; Fiske, S. J.; Hull, S. E.; Lessinger, L.; Germain, G.; DeClerq, J. P.; Woolfson, M. M. *MULTAN80: A System of Computer Programs for the Automatic Solution of Crystal Structures from X-Ray Diffraction Data*, University of York: England, 1980.

(38) Sheldrick, G. M. *Acta Crystallogr.* **1990**, *A46*, 467.

(39) The authors have deposited atomic coordinates for structures **1**–**5** with the Cambridge Crystallographic Data Centre. The coordinates can be obtained, on request, from the Director, Cambridge Crystallographic Data Centre, 12 Union Road, Cambridge, CB2 1EZ, UK.

Table 7. Crystallographic Data for Sulfones 1–5

	1	2	3	4	5
formula	$C_{20}H_{12}N_2O_2S$	$C_8H_4N_2O_2S$	$C_{16}H_{20}N_2O_2S$	$C_{18}H_{16}N_2O_2S$	$C_{18}H_{10}N_2O_2S_2$
formula wt	344.38	192.19	304.40	324.39	350.41
cryst syst	orthorhombic	monoclinic	orthorhombic	monoclinic	monoclinic
space group	*P*212121	*C*2	*Pnam*	*P*21/*n*	*P*21/*c*
a, Å	7.589(2)	8.964(2)	11.747(2)	13.370(5)	14.814(3)
b, Å	9.793(4)	8.907(2)	7.361(2)	9.914(2)	9.427(2)
c, Å	21.900(4)	11.173(2)	19.020(2)	12.570(5)	17.104(3)
α, deg	90.00	90.00	90.00	90.00	90.00
β, deg	90.00	113.66(3)	90.00	96.93(2)	137.16(3)
γ, deg	90.00	90.00	90.00	90.00	90.00
V, Å^3	1627.7(8)	817.1(3)	1644.7(7)	1654.0(10)	1624.1(6)
Z	4	4	4	4	4
cryst size, mm	0.28 × 0.24 × 0.17	0.15 × 0.15 × 0.13	0.38 × 0.36 × 0.36	0.43 × 0.30 × 0.28	0.25 × 0.10 × 0.08
d_{calcd}, g cm^{-3}	1.405	1.562	1.229	1.303	1.302
μ(Mo Kα), cm^{-1}	0.215	3.253[a]	0.203	0.206	1.859
rflns collected	1664	1471	1496	2295	2709
indep rflns	1659	667	1490	2295	2348
rflns obsd	1184	625	1072	1857	2021
R	0.050	0.052	0.046	0.050	0.046
R_w	0.109	0.141	0.124	0.115	0.134

[a] μ(Cu Kα).

The sample proper, typically 10-μm-thick, consisted of the electron-transport material (**3**, **4**, or **15**) molecularly dispersed in the polyester binder, poly[4,4′-(2-norbornylidene)bisphenol azelate-co-terephthalate (60/40)]. A solution of these components in CH_2Cl_2 (10% total solids by weight: 15% **3**, **4**, or **15**; 85% polymer) was coated with a doctor blade over the CGL and dried in air at 70 °C for 30 min. Dots of semitransparent Au, 5 mm in diameter, were evaporated onto the sample. Electrical contact was made to the aluminum and the gold layers. The capacitance between them was used to evaluate the thickness of the sample, assuming a dielectric constant of 3 and neglecting the thickness of the CGL.

The Au layer was connected to a high-voltage power supply via a relay. Flash illumination was provided by a xenon flash lamp, a long-pass (>540 nm) filter, and suitable neutral density filters. The voltage across a current-sensing resistor connected to the Al electrode was recorded with a Sony-Tektronix 390AD Programmable Digitizer and transferred to a 386 PC for further analysis. The current trace was smoothed and differentiated numerically, and tangents were drawn as illustrated in Figure 13. The crossing of the tangents was used as an operational definition of the transit time.[40]

Supplementary Material Available: Figures 15–18, which show absorption spectra for neutral **1**, **3**, **6**, and **2** and their one-electron reduction products, and Figures 19–21, which show the experimental and simulated EPR spectra for anion radicals of **1**, **3**, and **6** (7 pages). This material is contained in libraries on microfiche, immediately follows the article in the microfilm version of the journal, and can be ordered from the ACS; see any current masthead page for ordering information.

JO941786K

(40) Schein, L. B. *Philos. Mag. B* **1992**, *B65*, 795.